Research Article

Ashok Magar and Achchhe Lal*

Stress analysis of infinite laminated composite plate with elliptical cutout under different in plane loadings in hygrothermal environment

https://doi.org/10.1515/cls-2021-0001
Received Aug 01, 2020; accepted Nov 07, 2020

Abstract: This paper presents the solution of stress distribution around elliptical cutout in an infinite laminated composite plate. Analysis is done for in plane loading under hygrothermal environment. The formulation to obtain stresses around elliptical hole is based on Muskhelishvili's complex variable method. The effect of fibre angle, type of in plane loading, volume fraction of fibre, change in temperature, fibre materials, stacking sequence and environmental conditions on stress distribution around elliptical hole is presented. The study revealed, these factors have significant effect on stress concentration in hygrothermal environment and stress concentration changes are significant with change in temperature.

Keywords: stacking sequence, stress concentration, hygrothermal, complex variable

Nomenclature

$\sigma_x^\infty \sigma_y^\infty \tau_{xy}^\infty$	applied stresses at infinity
$\sigma_x \sigma_y \tau_{xy}$	stresses in Cartesian coordinates
$\sigma_r \sigma_\theta \tau_{r\theta}$	stresses in polar coordinates
$\varepsilon_x \varepsilon_x \varepsilon_{xy}$	strains in Cartesian coordinates
$[a_{i,j}]$	material property matrix
U	Airy's stress function
$\mu_1 \mu_2$	complex parameter
$a,\ b$	major and minor axis of ellipse
Z & ζ	complex variables in z & ζ plane
$\varphi(z_1),\ \psi(z_2)$	stress functions in z plane
λ	biaxial loading condition
$\varphi_1(z_1),\ \psi_1(z_2)$	first stage stress function
$\varphi_0(z_1),\ \psi_0(z_2)$	second stage stress function
$\varphi_0(\zeta),\ \psi_0(\zeta)$	second stage stress function in ζ plane
$f_1\ f_2$	hole reactions
H_1 *to* H_4	complex constants
$\overline{H_1}$ *to* $\overline{H_4}$	complex conjugate
E_{f1} and E_{f2}	the elastic module of fiber material along the fiber and transverse direction
ν_{f1} and ν_{f2}	Poisson ratios of fiber material along the fiber and transverse direction
V_f and V_m	fiber and matrix volume fraction
β_{f1} and β_{f2}	moisture coefficients of fiber along the fiber and transverse direction
$\alpha_{f1},\ \alpha_{f2}$	thermal expansion coefficients of fiber along x and y-direction
α_m and E_m	thermal expansion coefficient and modulus of elasticity of matrix material
β_m and V_m	moisture coefficient and volume fraction of matrix material
E_1 and E_2	modulus of elasticity along longitudinal and transverse direction of fiber
α_{11} and α_{22}	thermal expansion coefficients of laminated reinforced composite along x and y-direction
α_1	coefficient of thermal expansion of composite material
$x,\ y,\ z$	cartesian coordinates
ΔT	increment in temperatures
ΔC	increment in moisture

***Corresponding Author: Achchhe Lal:** Department of Mechanical Engineering, S.V. National Institute of Technology Surat, Keval Chowk, Surat, Gujarat 395007, India;
Email: achchhelal@med.svnit.ac.in, lalachchhe@yahoo.co.in;
Tel.: 0261-220-1993
Ashok Magar: Department of Mechanical Engineering, S.V. National Institute of Technology Surat, Keval Chowk, Surat, Gujarat 395007, India; Email: ashok.magar@gmail.com

1 Introduction

The use of the laminated composite plates has extensively increased in advanced and modern engineering applications. It is due to the fact that composite laminates possesses very high strength to weight and stiffness to strength ratio. Due to these excellent properties, composite laminate

structures are light in weight and give superior performance in structural engineering applications and are very popular in weight sensitive applications like spacecrafts. As a part of service requirement in certain applications, holes or cutouts are made in the structures. When these structures with holes or openings are subjected to different types of loadings, they give rise to stress concentrations. In engineering applications like pressure vessels, openings of circular or elliptical shape, they are provided for inspection purpose. Window structure in aeroplanes is one of the examples of service requirement. Stress investigation of infinite plates with holes or opening or cutouts is an interesting area of analysis. Investigation is needed to study the effect of loading, environmental conditions, like temperature and moisture, etc. on stress concentration. Better estimation of stress concentration factor helps to improve optimum performance of structures made from composite laminates. Stress concentration around elliptical holes plays an important role in the failure and fracture of the structures.

Savin [1] obtained the solution for stress distribution around circular, elliptical, triangular and rectangular holes in isotropic as well as anisotropic plates using Mushkhelisvili's complex variable. Daoust *et al.* [2] analyzed stress distribution around a triangular hole in anisotropic material and revealed the effect of length/height ratios of the triangular hole, degrees of bluntness at the triangle vertex and load orientation on stress concentration. Xin Lin Gao [3] solved problem of infinite isotropic plate with elliptical hole and revealed effect of arbitrary biaxial loadings on stress concentration. Simha *et al.* [4] analyzed stress concentration around irregular hole having fixed hole geometry with perimeter being varied and subjected to different in plane loading. Theocaris *et al.* [5] investigated triangular hole under tension at infinity. Effect of round of corners on stress concentration was revealed. Kakhandki *et al.* [6] revealed stress distribution around irregular shaped hole in an orthotropic laminate using savin's approach. The results are validated with the FEM solution. Rao *et al.* [7] used Savin formulation to get stresses around holes in anisotropic plates under inplane loading. It considers the effect of arbitrary shape of hole and arbitrarily oriented loading. Failure strength of the laminate is also obtained using different laminate failure criterion. Jafari *et al.* [8] revealed the effect of varying parameters, like cutout shape and bluntness, load direction or cutout orientations on the stress distributions and SCF in the perforated plates. Sharma and Dave [9] obtained general solution to SIF for hypocycloidal hole in infinite symmetric anisotropic plate. Study revealed effect of stacking sequence, hole geometry, material properties and loading angle on stress intensity factors for hypocycloidal hole. Darwish *et al.* [10] investigated stress concentration factor (SCF) in countersunk rivet holes in orthotropic laminated plates subjected to uniaxial tension. The effect of geometric and material parameters such as plate thickness, straight-shank radius, countersunk angle, countersunk depth, plate width, and the laminate ply angles on the SCF is investigated. A relation fitting in these parameters is obtained to get SCF around rivet hole. Patel *et al.* [11] revealed the effect of stacking sequence, ply groups, loading angles, materials and corner radii on the failure strength and moment distribution in symmetric laminated composite plate containing a square hole. The layer wise stresses and failure strengths are evaluated and the failure strengths of laminates are calculated. Khamseh and Waas [12] done the experimental analysis to investigate failure mechanisms in laminated composite plates containing circular cutouts, under biaxial in plane compressive loading. Biaxial tests were carried out with 48 ply graphite/epoxy composites by varying fibre orientation. Sharma [13] investigated an optimum design of a 4, 8 and 16 layered graphite/epoxy and glass/epoxy symmetric laminated plate containing an elliptical hole subjected to in-plane loading conditions using complex variable method and genetic algorithm (GA). The optimum stacking sequence is obtained using genetic algorithm. Li *et al.* [14] investigated a plate weakened by an oblique penetration of a circular cylindrical hole using finite element method. Parametric studies of effects of angle of inclination, plate thickness, and width are revealed & empirical relation is developed. Hasebe *et al.* [15] investigated the problem of a crack originated at point of a circular hole with rigidly stiffened displacement. For this case stress distributions and SIF are calculated using complex variable method. Puhui *et al.* [16] investigated stresses around elliptic hole using, Lekhnitskii's complex potential method in unsymmetric composite laminate plate. W. Becker *et al.* [17], solved a problem of finding moments around elliptical hole in unsymmetric laminate plate. The new complex potential is developed.

Many researchers have investigated the effect of environmental conditions on the behaviour of laminated composite plate. Analytical results using Chebyshev series for the non-linear flexural response of hygrothermomechanical loaded elastically supported thick laminated rectangular plates were investigated by Upadhyay *et al.* [18]. Buckling behaviour of the composite laminate plate under hygrothermo mechanical loading was analyzed using C^0 FEM by Kumar *et al.* [19]. Non-linear static behaviour of a piezoelectric sandwich plate having elastic foundation and hygrothermo mechanical loading was investigated by Lal *et al.* [20] by using SFSDT and investigated the ef-

fect of random system characteristics with fibre volume fraction, stacking sequence, type of geometry, etc. on the transverse largest deflection. Static analysis of a sandwich plate having a soft compressible core was revealed by a higher-order Zig-zag theory by Pandit *et al.* [21]. Hadjiloizi *et al.* [22, 23] build a micro-mechanical model to analyze smart composite magnato-thermoelastic thin plate with varying thickness using 3D formulation in Part-I [22]. In second part [23], the theory is applied using examples of thin laminated magnetoelectric plates having constant thickness. Hsieh [24] investigated the effect of heat flow and moisture transfer on stresses and moments around elliptical hole in composite plate. Rahnama [25] investigated SCF in unidirectional composite plate having broken fibres and hygrothermal condition. Effect of fibre volume fraction on SCF in wet and dry conditions is studied. Sai Ram [26] analyzed moments around cutouts in hygrothermal environment with transverse loading in unsymmetric laminate plate.

Dimitri *et al.* [27] used SFEM and IGA to obtain SCF in isotropic plates with inclusions like circular holes, u and v notches. Fantuzzi *et al.* [28] obtained numerically mode I SIF in composite structures using SFEM based on GDQ method. SFEM with domain decomposition technique is used by Viola *et al.* [29] to study stresses in infinite plate with circular inclusions and uniaxial loading.

From the literature survey, it is observed that the researches have done the work on the analysis of laminated composite plates containing cutouts of different shapes and subjected to inplane moments or forces to get stresses and bending moments around cutouts. Hygrothermal effects on SCF are investigated by number of researchers by considering transverse loading. To the best of the author's knowledge for in plane loading, effect of various parameters like stacking sequence, fiber orientation, loading conditions, fiber volume fraction, and cutout dimensions on the normalized stresses around elliptical hole under hygrothermal conditions were not investigated.

In the current analysis stress distribution around elliptical hole in composite laminate subjected to in plane loading is investigated. The effect of laminate stacking sequence, fiber orientation, loading conditions, fiber volume fraction, type of fibre material under hygrothermal conditions on stresses around elliptical cutout is studied.

2 Mathematical formulation

An anisotropic infinite plate with an elliptical cutout having major axis as a & minor axis as b is subjected to in plane loading at infinity as shown in Figure 1. To account for all cases of loading, general loading condition of Gao [3] is considered. λ is a loading factor & β is angle made by X'Y' coordinate system with XY coordinate system. Figure 2 shows different in plane loading cases considered in present analysis by choosing appropriate λ and β.

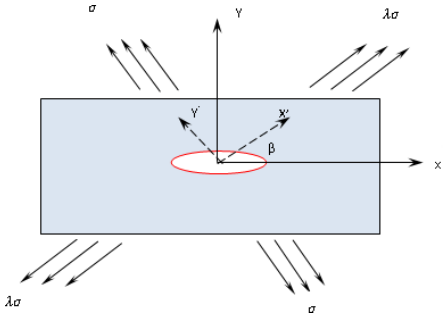

Figure 1: Infinite plate with elliptical shape cutout subjected to in plane loading

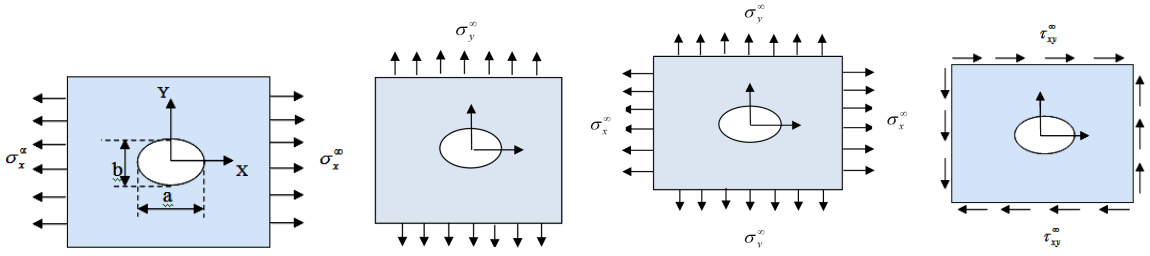

(a) Tensile loading in x direction at infinity, Loading factor, $\lambda = 0, \beta = \frac{\pi}{2}$

(b) Tensile loading in y direction at infinity, Loading factor, $\lambda = 0, \beta = 0$

(c) Biaxial tension at infinity, Loading factor, $\lambda = 1, \beta = 0$

(d) Shear loading at infinity, Loading factor, $\lambda = -1\ \beta = \frac{\pi}{4}$

Figure 2: Loading factor λ and β for different in plane loading

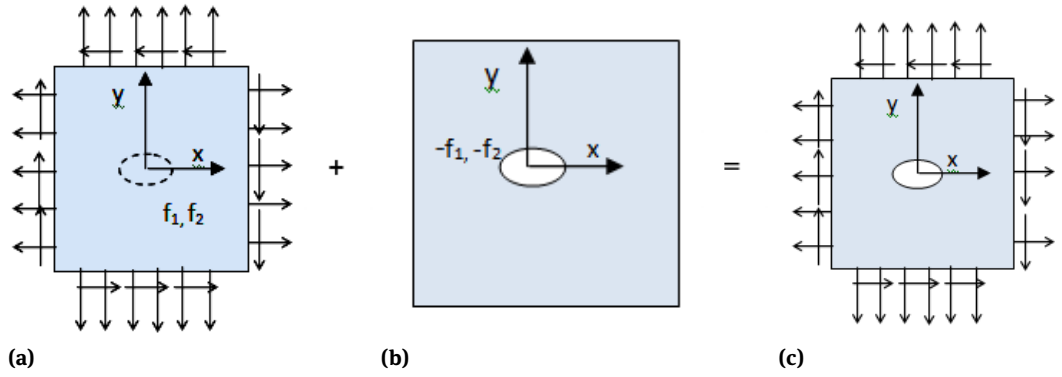

Figure 3: Solution scheme: a) Plate without hole & loading at infinity; b) Plate with negative of boundary condition at hole boundary; c) Plate with eliptical hole & loading at infinity.

2.1 Complex variable representation

Plate thickness is very small as compared with other two dimensions and loading is in plane hence approximating problem as plane stress problem with stresses in out of plane direction as zero. Plate faces are stress free. The generalized Hooke's law for a thin anisotropic plate for arbitrary loading along X'Y' axis relates stresses σ_x, σ_y, τ_{xy} and strains ϵ_x, ϵ_y, ϵ_{xy},

$$\{\sigma\}^T = [a_{ij}]\{\varepsilon\}^T \quad where, \quad i,j = 1,2,6 \tag{1}$$

$[a_{ij}]$ For the multilayer laminate with given fiber orientation angle is calculated using method given in [30].

The stresses in terms of the Airy's stress function U are given by,

$$\sigma_x = \frac{\partial^2 U}{\partial y^2}, \quad \sigma_y = \frac{\partial^2 U}{\partial x^2}, \quad \tau_{xy} = \frac{\partial^2 U}{\partial x \partial y} \tag{2}$$

Keeping Eq. (2) in Eq. (1) & putting the result in compatibility equation, we get the 4^{th} order biharmonic characteristic equation of the system.

$$a_{11}\mu^4 - 2a_{16}\mu^3 + (2a_{12} + a_{66})\mu^2 - 2a_{16}\mu + a_{22} = 0 \tag{3}$$

The Eq. (3) has four roots (μ_j $j = 1,2,3,4$) whose values depends on $[a_{ij}]$ are known as complex parameters. Using Muskhelishvili's complex variable approach [32], the stress components in XY plane are given by,

$$\begin{aligned} \sigma_x &= 2\mathrm{Re}\left(\mu_1^2\varphi'(z_1) + \mu_2^2\psi'(z_2)\right) \\ \sigma_y &= 2\mathrm{Re}\left(\varphi'(z_1) + \psi'(z_2)\right) \\ \tau_{xy} &= -2\mathrm{Re}\left(\mu_1\varphi'(z_1) + \mu_2\psi'(z_2)\right) \end{aligned} \tag{4}$$

To get stress functions $\varphi(z_1)$ & $\psi(z_2)$, conformal mapping is used. The area outside the elliptical hole with major diameter a & minor diameter b in z plane is mapped outside the circle having unit radius in ζ plane using mapping function $\omega(\zeta)$,

$$z = \omega(\zeta) = R\left(\zeta + m\zeta^{-1}\right), \text{ where } m = \frac{a-b}{a+b}, \tag{5}$$

R is size factor

For unit circle, $\zeta = \cos\theta + i\sin\theta$, using in Eq. (5) along with complex parameter μ_1 and μ_2, we get final mapping function,

$$z_j = \omega_j(\zeta) = \frac{R}{2}\left(a_j\left(\zeta^{-1} + m\zeta\right) + b_j\left(\zeta + m\zeta^{-1}\right)\right), \tag{6}$$

$j = 1,2$

Where

$$a_j = 1 + i\mu_j, \quad b_j = 1 - i\mu_j \tag{7}$$

Stress function $\varphi(z_1)$ & $\psi(z_2)$ are obtained by using superposition principle as shown in Figure 3. In first stage, the plate with the fictitious hole is considered and first stage stress functions $\varphi_1(z_1)$ and $\psi_1(z_2)$ are obtained using boundary conditions shown in Figure 3a. First stage stress functions are used to find the boundary conditions f_1 and f_2 at hole boundary. In second stage, negative of f_1 and f_2 are applied at hole boundary Figure 3b and second stage stress function $\varphi_0(z_1)$ and $\psi_0(z_2)$ are obtained. As seen in Figure 3c, addition of first & second stage gives original configuration of infinite plate with hole subjected to loading at infinity.

As per superposition principle,

$$\begin{aligned} \varphi(z_1) &= \varphi_1(z_1) + \varphi_0(z_1) \\ \psi(z_2) &= \psi_1(z_2) + \psi_0(z_2) \end{aligned} \tag{8}$$

Stress function for first stage is given by,

$$\begin{aligned} \varphi_1(z_1) &= Bz_1 \\ \psi_1(z_2) &= \left(B^* + iC^*\right)z_2 \end{aligned} \tag{9}$$

Using Gao's [3] biaxial loading factor λ, stresses applied at infinity along X'& Y' axis are given by, (refer to Figure 1)

$$\sigma_{x'}^{\infty} = \lambda\sigma \quad \sigma_{y'}^{\infty} = \sigma \quad \tau_{x'y'}^{\infty} = 0 \tag{10}$$

Putting Eq. (9) in Eq. (4) and solving Eq. (4) simultaneously to get constants B, B* & C*.

The boundary condition in stage 1 are given by

$$\begin{aligned} f_1 &= 2\mathrm{Re}\left[\varphi_1(z_1) + \psi_1(z_2)\right] \\ f_2 &= 2\mathrm{Re}\left[\mu_1\varphi_1(z_1) + \mu_2\psi_1(z_2)\right] \end{aligned} \tag{11}$$

Keeping Z_1 and Z_2 from Eq. (6) into Eq. (9) and using Eq. (9) in Eq. (11) we get

$$\begin{aligned} f_1 &= \left[\left(H_1 + \overline{H_2}\right)\left(\zeta^{-1} + m\zeta\right)\right. \\ &\quad \left. + \left(H_1 + \overline{H_2}\right)\left(\zeta + m\zeta^{-1}\right)\right] \\ f_1 &= \left[\left(H_3 + \overline{H_4}\right)\left(\zeta^{-1} + m\zeta\right) + \left(H_3 + \overline{H_4}\right)\left(\zeta + m\zeta^{-1}\right)\right] \end{aligned} \tag{12}$$

Where,

$$\begin{aligned} H_1 &= \frac{R}{2}\left[Ba_1 + \gamma a_2\right] \quad H_2 = \frac{R}{2}\left[Bb_1 + \gamma b_2\right] \\ H_3 &= \frac{R}{2}\left[\mu_1 Ba_1 + \mu_2\gamma a_2\right] \quad H_4 = \frac{R}{2}\left[\mu_1 Bb_1 + \mu_2\gamma b_2\right] \\ \text{and} \quad \gamma &= B^{*} + iC^{*} \end{aligned} \tag{13}$$

Negative of boundary condition is, $-f_1 = f_1^0$ and $-f_2 = f_2^0$

Stress functions of second stage are obtained by using Schwarz formula [1]

$$\begin{aligned} \varphi_0(\zeta) &= \frac{i}{4\pi(\mu_1 - \mu_2)} \int_{\Gamma} \left(\mu_2 f_1^0 - f_2^0\right)\left(\frac{t+\zeta}{t-\zeta}\frac{dt}{t}\right) \\ &\quad + \lambda_1 \\ \psi_0(\zeta) &= \frac{-i}{4\pi(\mu_1 - \mu_2)} \int_{\Gamma} \left(\mu_1 f_1^0 - f_2^0\right)\left(\frac{t+\zeta}{t-\zeta}\frac{dt}{t}\right) + \lambda_2 \end{aligned} \tag{14}$$

Γ is boundary of unit circle in ζ plane and λ_1 and λ_2 are complex constants and does not affect stress solution hence removed from the equation.

Keeping $-f_1 = f_1^0$ and $-f_2 = f_2^0$ in Eq. (14) and evaluating integral we get

$$\begin{aligned} \varphi_0(\zeta) &= \left[a_2\zeta^{-1} + b_3 m\zeta^{-1}\right] \\ \psi_0(\zeta) &= \left[a_4\zeta^{-1} + b_4 m\zeta^{-1}\right] \end{aligned} \tag{15}$$

$$\begin{aligned} a_3 &= s\left[\mu_2\left(H_1 + \overline{H_2}\right) - \left(H_3 + \overline{H_4}\right)\right] \\ b_3 &= s\left[\mu_2\left(H_2 + \overline{H_1}\right) - \left(H_4 + \overline{H_3}\right)\right] \\ a_4 &= s\left[\mu_1\left(H_1 + \overline{H_2}\right) - \left(H_3 + \overline{H_4}\right)\right] \\ b_4 &= s\left[\mu_1\left(H_2 + \overline{H_1}\right) - \left(H_4 + \overline{H_3}\right)\right] \end{aligned} \tag{16}$$

Where, $s = \frac{1}{\mu_1 - \mu_2}$

Keeping values from Eq. (9) & Eq. (15) in Eq. (8) we get stress functions $\varphi(z_1)$ and $\psi(z_1)$. Putting these stress function in Eq. (4), we get the following equations of stresses around the hole.

$$\begin{aligned} \sigma_x &= \sigma_x^{\infty} + 2\mathrm{Re}\left[\mu_1^2\varphi_0'(z_1) + \mu_2^2\psi_0'(z_2)\right] \\ \sigma_y &= \sigma_y^{\infty} + 2\mathrm{Re}\left[\varphi_0'(z_1) + \psi_0'(z_2)\right] \\ \tau_{xy} &= \tau_{xy}^{\infty} - 2\mathrm{Re}\left[\mu_1\varphi_0'(z_1) + \mu_2\psi_0'(z_2)\right] \end{aligned} \tag{17}$$

To get $\varphi_0'(z_1)$ and $\psi_0'(z_2)$ in z plane (in Eq. 17) from $\varphi_0(\zeta)$ and $\psi_0(\zeta)$ in ζ plane, following transformation equations are used,

$$\begin{aligned} \varphi_0'(z_1) &= \frac{\varphi_0'(\zeta)}{\omega_1'(\zeta)} \quad \psi_0'(z_2) = \frac{\psi_0'(\zeta)}{\omega_2'(\zeta)} \\ \omega_1'(\zeta) &= \frac{dz_1}{d\zeta} \quad \omega_2'(\zeta) = \frac{dz_2}{d\zeta} \end{aligned} \tag{18}$$

To transform stresses from Cartesian coordinate system (Eq. (17)) to polar coordinate system, following transformation equations are used.

$$\begin{aligned} \sigma_\theta + \sigma_r &= \sigma_x + \sigma_y, \\ \sigma_\theta - \sigma_r + 2i\tau_{r\theta} &= e^{2i\phi}\left(\sigma_y - \sigma_x + 2i\tau_{xy}\right) \end{aligned} \tag{19}$$

2.2 Properties of laminate

The micromechanical approach is used in the present paper to get the material properties of the composite laminates to account the effect of temperature and environment conditions. The properties retention ratio for the matrix is given as [20]

$$R_m = \left[\frac{t_w - t}{t_d - t_{env}}\right]^{\frac{1}{2}} \tag{20}$$

Where, t is the temperature at which properties of a composite laminate is to be estimated, t_d, t_{evn} and t_w are glass transition temperature for dry condition, reference environmental temperature and glass transition temperature at wet conditions respectively.

Using the micromechanical approach, the elastic constants of reinforced composite laminate are given by following equations [20]

$$E_{11} = E_{f1}V_f + R_m E_m V_m \tag{21}$$

$$E_{22} = \left(1 - \sqrt{V_f}\right)R_m E_m + \frac{R_m E_m \sqrt{V_f}}{1 - \sqrt{V_f}\left(1 - \frac{R_m E_m}{E_{f2}}\right)} \tag{22}$$

$$G_{12} = \left(1 - \sqrt{V_f}\right)R_m G_m + \frac{R_m G_m \sqrt{V_f}}{1 - \sqrt{V_f}\left(1 - \frac{R_m G_m}{G_{f12}}\right)} \tag{23}$$

$$\nu_{12} = \nu_{f12} V_f + \nu_m V_m \tag{24}$$

Where 'f' and 'm' are subscript used for fiber and matrix material of composite lamina. The matrix thermal property can be estimated with a thermal characteristics retention ratio given as

$$F_{th} = \frac{1}{F_m} \tag{25}$$

The thermal expansion coefficients using a micromechanical approach can be written as Kumar *et al.* [19]

$$\alpha_{11} = \frac{E_{f1} V_f \alpha_{f1} + F_m E_m V_m F_{th} \alpha_m}{E_{f1} V_f + F_m E_m V_m} \tag{26}$$

$$\alpha_{22} = \left(1 + \nu_{f12}\right) V_f \alpha_{f2} + (1 + \nu_m) V_m F_{th} \alpha_m - \nu_{12} \alpha_{11} \tag{27}$$

3 Results and discussion

In the present solution, stresses around the elliptical hole in an infinite symmetric laminate plate subjected to in plane loading at infinity is obtained. The cross and angle ply laminates along with different stacking sequences are considered for the analysis.

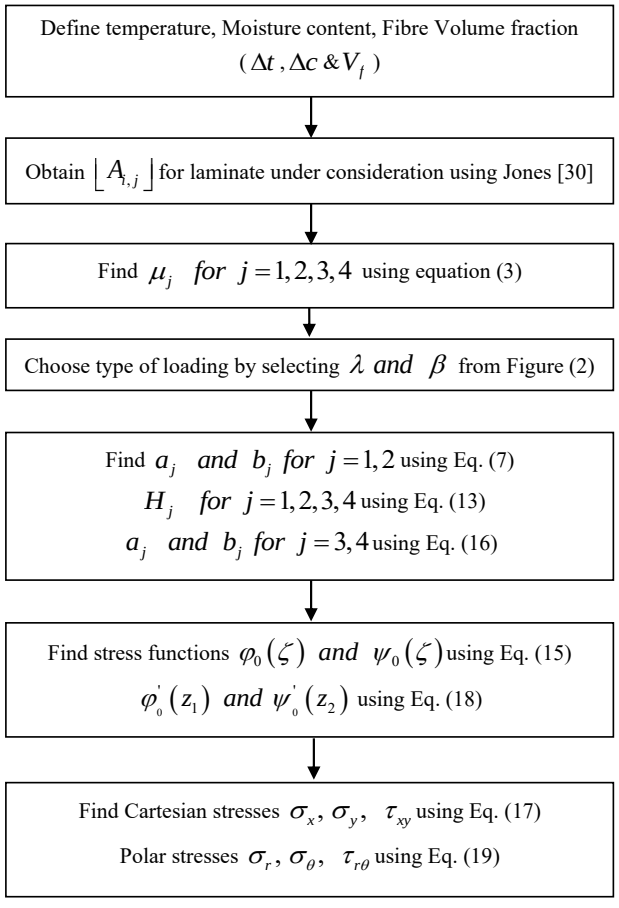

Figure 4: Flow chart indicating steps in finding stresses around elliptical hole.

The material properties of composite laminate used in the present paper are obtained by using micromechanical approach to account for temperature & environment effects.

Flow chart in Figure 4 gives procedure of getting stress distribution around elliptical cutout under hygrothermal environment.

Properties of carbon fiber (T-300) & matrix material listed below are used for calculating stress distribution results around the elliptical hole.

$E_{f1} = 220 \times 10^9 \text{Pa}$, $E_{f2} = 13.79 \times 10^9 \text{Pa}$, $\nu_{f12} = 0.2$,
$\alpha_{f1} = -0.99 \times 10^{-6} \text{m/°C}$, $\alpha_{f2} = 10.08 \times 10^{-6} \text{m/°C}$,
$\nu_{f12} = 0.25$, $E_m = 3.45 \times 10^9 \text{Pa}$, $\nu_m = 0.35$,
$\alpha_m = 72 \times 10^{-6} m/°\text{C}$, $\beta_m = 0.33$ mm/% RH ,
$\beta_{f1} = \beta_{f2} = 0$ mm/% RH,

The effects of loading, materials, temperature, humidity, fiber volume fraction, laminate geometry and stacking sequence of lamina on stress distribution around the elliptical hole can be analyzed effectively by using the solution presented in this paper.

Figure 5(a) shows the results of stress distribution around elliptical hole in 16 ply laminate plate of Graphite epoxy, subjected to equibiaxial tension $\sigma_x^\infty = \sigma_x^\infty = 1$. The maximum tangential stress, $\sigma_{\theta max} = 3.8588$ occur at 4.5° & 184.5° which is in good agreement with result presented in Sharma [11]. Figure 5(b) shows the stress distribution results from Sharma [11].

Figure 6 shows the variation in σ_θ around elliptical hole due to temperature change in [0/90]s laminate. The maximum values of tangential stresses are, $\sigma_{\theta max} = 9.8190$, 10.3304, 11.1480, 12.8781 for $\Delta t = 0°$, 50°, 100°, 150°. These values occur at 0° & 180° angle as expected for cross ply laminate. For $\Delta t = 150°$, percentage change in $\sigma_{\theta max}$ is 31.15% & for $\Delta t = 50°$ it is 4.85%. So it is clear that for higher temperature rise effect on stress concentration is significant.

Table 1 depicts the variations in $\sigma_{x\max}$ $\sigma_{y\max}$ $\tau_{xy\max}$ due to the change in the temperature Δt. Cross ply laminate with elliptical hole having a/b=2 is subjected to equibiaxial tenstion. Shear stress $\tau_{xy\max}$ is least affected due to change in the temperature. The Location of these maximum stresses for given loading condition are different.

Laminate plate with elliptical hole is subjected to equiaxial loading and results for $\sigma_{\theta\max}$ listed in Table 2. From Table 2, it is clear that stacking sequence affect the $\sigma_{\theta\max}$ considerably. To limit the stress concentration for a given loading, selection of proper lamina angles and stack-

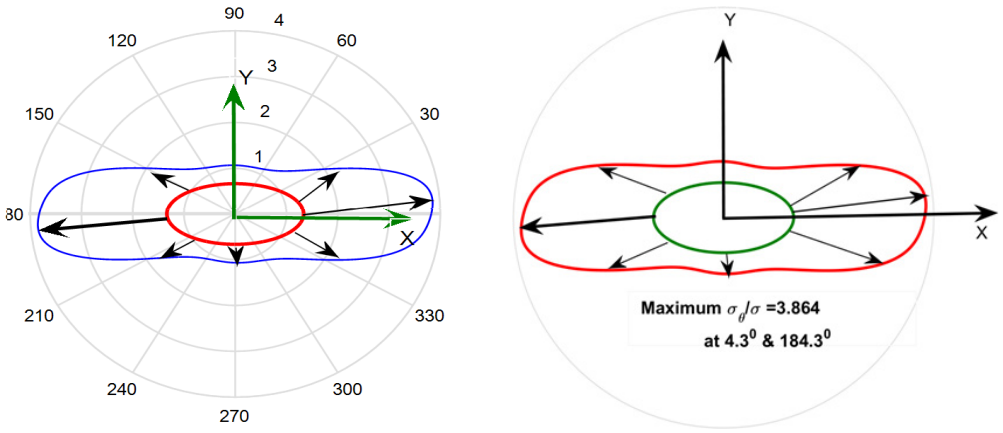

(a) (b)

Figure 5: Stress distribution around elliptical hole in composite laminate plate subjected to equibiaxial tension with stacking sequence $[-43.3204871^\circ/88.4927171^\circ/34.1990231^\circ/45.1948441^\circ/-68.3984651^\circ/-89.9608541^\circ/73.1113401^\circ/-43.0827171^\circ]_s$ (a) Present solution and (b) Sharma [11]

Table 1: Effect of Δt on $\sigma_{x\,\max}$ $\sigma_{y\,\max}$ $\tau_{xy\,\max}$ (a/b = 2, $\sigma_x^\infty = \sigma_y^\infty = 1$, [0/90]s)

Δt	$\sigma_{x\,\max}$	**Angle for** $\sigma_{x\,\max}$	$\sigma_{y\,\max}$	**Angle for** $\sigma_{y\,\max}$	$\tau_{xy\,\max}$	**Angle for** $\tau_{xy\,\max}$
0	2.4548	90° & 270°	9.8190	0° & 180°	1.0547	174° & 354°
50	2.5826		10.3304		1.0493	
100	2.7870		11.1480		1.0420	
150	3.2195		12.8781		1.0310	

Table 2: Effect of Δt and stacking sequence on $\sigma_{\theta\,\max}$ (a/b = 2, $\sigma_x^\infty = \sigma_x^\infty = 1$)

Δt	**[0/90/0/90]s**	**[45/−45]s**	**[30/45/60/90]s**	**[0/45/45/90]s**	**[45/90/90/45]s**
0	9.8190	5.6450	5.2539	4.7537	6.1392
50	10.3304	5.9209	5.3669	4.7872	6.3514
100	11.1480	6.3735	5.5432	4.8341	6.6993
150	12.8781	7.3220	5.8943	4.9120	7.4656

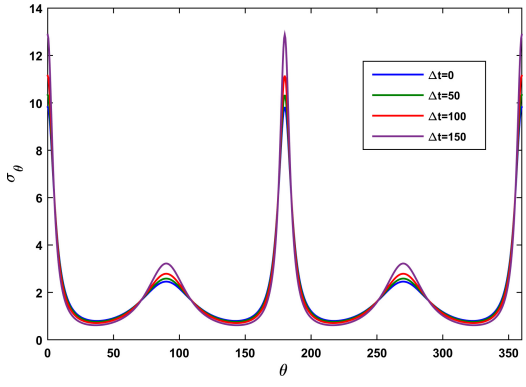

Figure 6: Effect of Δt on σ_θ around elliptical hole in orthotropic plate subjected to $\sigma_x^\infty = \sigma_x^\infty = 1$

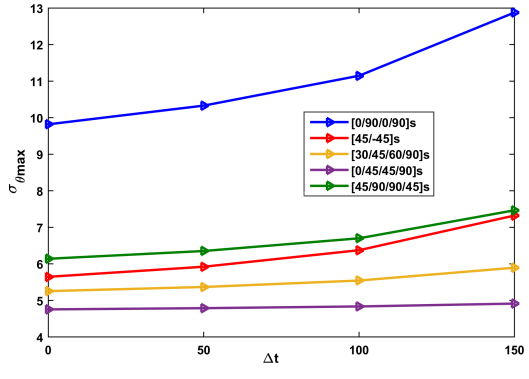

Figure 7: Effect of Δt on $\sigma_{\theta\,\max}$ around elliptical hole in orthotropic plate subjected to for different stacking sequence and lamina fibre orientation

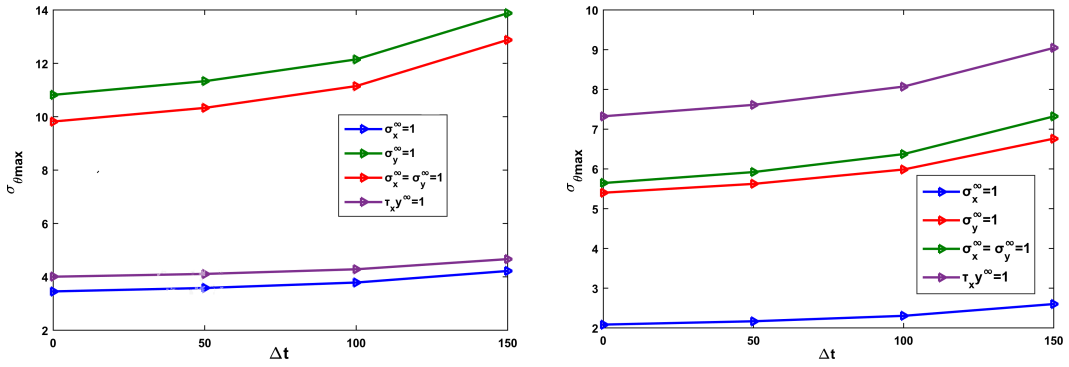

Figure 8: Effect of Δt on $\sigma_{\theta\,\max}$ around elliptical hole in orthotropic plate for different in plane loadings (a) Cross ply [0/90]s (b) Angle ply [45/−45]s

Table 3: Effect of Δt and load angle on $\sigma_{\theta max}$ (a/b = 2, Load angle variation from 0° to 90° axis, [0/90]s)

Load angle	$\Delta t = 0°$		$\Delta t = 50°$		$\Delta t = 100°$		$\Delta t = 150°$	
	$\sigma_{\theta\,\max}$	Angle for $\sigma_{\theta\,\max}$	$\sigma_{\theta\,\max}$	Angle for $\sigma_{\theta\,\max}$	$\sigma_{\theta\,\max}$	Angle for $\sigma_{\theta\,\max}$	$\sigma_{\theta\,\max}$	Angle for $\sigma_{\theta\,\max}$
0	3.4548	90° & 270°	3.5826	90° & 270°	3.7870	90° & 270°	4.2195	90° & 270°
10	3.4463	85° & 265°	3.5733	85° & 265°	3.7768	85° & 265°	4.2074	85° & 265°
20	3.3922	81° & 261°	3.5158	81° & 261°	3.7139	81° & 261°	4.1357	81° & 261°
30	3.2349	77° & 257°	3.3503	77° & 257°	3.5361	77° & 257°	3.9332	77° & 257°
40	4.6988	2.5° & 182.5°	4.9175	2.5° & 182.5°	5.2643	2.5° & 182.5°	6.0066	2.5° & 182.5°
50	6.5146	2° & 182°	6.8130	2° & 182°	7.3120	2° & 182°	8.3351	2° & 182°
60	8.2096	1.5° & 181.5°	8.5960	1.5° & 181.5°	9.2235	1.5° & 181.5°	10.5325	1.5° & 181.5°
70	9.5946	1° & 181°	10.0392	1° & 181°	10.7694	1° & 181°	12.3152	1° & 181°
80	10.5027	0.5° & 180.5°	10.9964	0.5° & 180.5°	11.7839	0.5° & 180.5°	13.4425	0.5° & 180.5°
90	10.8190	0° & 180°	11.3304	0° & 180°	12.1480	0° & 180°	13.8781	0° & 180°

ing sequence is very important. The variation in stress concentration due to change in temperature is 31% & 29% respectively for first two ply groups with $\Delta t = 150°$. From Figure 7, it is clear that stacking sequence has significant effect on stress concentration with change in temperature. So selection of proper stacking sequence and lamina fibre orientation is required to minimize the effect of change in temperature on stress concentration. The stacking sequence affects the laminate properties and hence the stresses around the hole.

Figure 8a, 8b shows the effect of change in temperature on stress concentration in a cross ply and angle ply laminate plate subjected to uniaxial tension in x and y direction , biaxial tension and shear loading at infinity. From Figure8a it is clear that, for tensile loading in x direction & shear loading at infinity in cross ply laminate has least effect on stress concentration due to change in temperature. In cross ply laminate subjected to tensile loading along y axis or equibiaxial tensile loading, there is increase in stress concentration by 28% and 31% respectively. Figure8b depicts the effect of temperature change on stress concentration for angle ply laminate. For tensile loading in x direction variation in stress concentration is less but for other three types of loading it is considerable. From Figure8a and8b it is also clear that type of loading and fibre orientation has significant effect on stress concentration. Stress concentration in angle ply is less as compared with cross ply for different in plane loading.

Table 3 lists the results of $\sigma_{\theta\,\max}$ for a cross ply laminate subjected to tensile loading with load angle varied

Table 4: Effect of Δt and load angle on $\sigma_{\theta max}$ (a/b = 2, Load angle variation from 0° to 90° axis, [45/−45]s)

Load angle	$\Delta t = 0°$		$\Delta t = 50°$		$\Delta t = 100°$		$\Delta t = 150°$	
	$\sigma_{\theta\,\max}$	Angle for $\sigma_{\theta\,\max}$	$\sigma_{\theta\,\max}$	Angle for $\sigma_{\theta\,\max}$	$\sigma_{\theta\,\max}$	Angle for $\sigma_{\theta\,\max}$	$\sigma_{\theta\,\max}$	Angle for $\sigma_{\theta\,\max}$
0	2.0836	34.5° & 214.5°	2.1673	34.5° & 214.5°	2.3040	34.5° & 214.5°	2.6004	34.5° & 214.5°
10	3.0011	31° & 211°	3.1300	31° & 211°	3.3386	31° & 211°	3.7801	31° & 211°
20	4.0657	29° & 209°	4.2438	29° & 209°	4.5315	29° & 209°	5.1384	29° & 209°
30	5.1444	27° & 207°	5.3725	27° & 207°	5.7369	27° & 207°	6.5057	27° & 207°
40	6.0814	26° & 206°	6.3518	26° & 206°	6.7840	26° & 206°	7.6985	26° & 206°
50	6.7435	25.5° & 205.5°	7.0414	25.5° & 205.5°	7.5153	25.5° & 205.5°	8.5263	25.5° & 205.5°
60	7.0263	24.5° & 204.5°	7.3319	24.5° & 204.5°	7.8289	24.5° & 204.5°	8.8731	24.5° & 204.5°
70	6.8853	24°& 204°	7.1826	24°& 204°	7.6614	24°& 204°	8.6792	24°& 204°
80	6.3231	23° & 203°	6.5924	23° & 203°	7.0216	23° & 203°	7.9511	23° & 203°
90	5.4013	22.5°& 202.5°	5.6236	22.5°& 202.5°	5.9856	22.5°& 202.5°	6.7619	22.5°& 202.5°

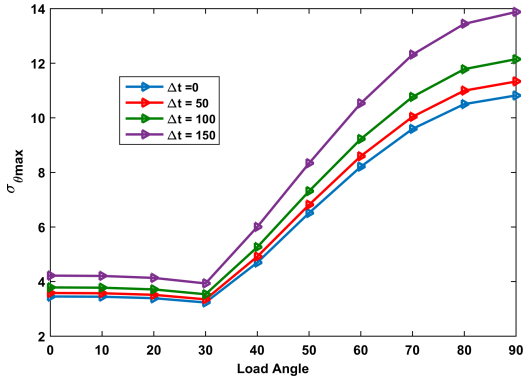

Figure 9: Effect of and load angle on $\sigma_{\theta\,\max}$ (a/b = 2, Load angle variation from 0° to 90° axis, [0 /90]s)

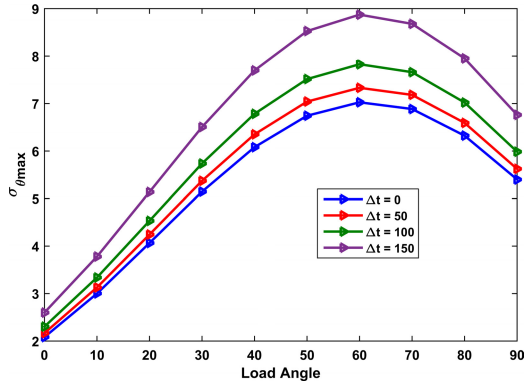

Figure 10: Effect of Δt and load angle on (a/b = 2, Load angle variation from 0° to 90° axis, [−45 /45]s)

from 0° to 90°. From table it is clear that, the location of $\sigma_{\theta\,\max}$ varies with the change in loading angle in x direction. From Figure 9 it is clear that, in cross ply laminate $\sigma_{\theta\,\max}$ decreases up to 30° loading angle & then increases. For a temperature change of above 100° effect on stress concentration is significant.

Table 4 shows the results of $\sigma_{\theta\,\max}$ for a angle ply laminate subjected to tensile loading with load angle varied from 0° to 90°. From Figure 10 it is clear that, in angle ply laminate $\sigma_{\theta\,\max}$ increases up to 60^0loading angle & then decreases. Comparing Table 3 & Table 4 along with Figure 9 and 10, it is observed that, effect of loading angle and temperature change is more significant in cross ply laminate as compared with angle ply laminate.

Table 5 shows the effect of fibre fraction on $\sigma_{\theta\,\max}$ for different values of Δt. Results are obtained for cross and angle plate laminate subjected to tensile loading along x axis ($\sigma_x^{\infty} = 1$). From the Table 5, it is clear that volume fraction of a fibre has a least effect on stress concentration as compared with the change in temperature. If fibre fraction is increased from 0.4 to 0.8 at $\Delta t = 0°$, there is 4.5 % change in the $\sigma_{\theta\,\max}$ but for Vf =0.1 & Δt changed from 0° to 150° there is 24% change in the $\sigma_{\theta\,\max}$.

Table 6 contains the results of moisture content effect on the $\sigma_{\theta\,\max}$. Cross ply and angle ply laminate plates subjected to tensile loading along x axis, y axis and biaxial loading is considered. From the Table 6, it is clear that change in moisture content has less effect on stress concentration for the cases of different types of stacking sequences, loading. For tensile loading along x direction, there is 0.26% change in stress concentration if Δc is varied from 0 to 0.2.

Table 5: Effect of fibre volume fraction and temperature on $\sigma_{\theta\max}$ ($\sigma_x^{\infty} = 1$, a/b = 2, [45/−45]s & [0/90]s)

	$\Delta t = 0°$		$\Delta t = 50°$		$\Delta t = 100°$		$\Delta t = 150°$	
Vf	$\sigma_{\theta\max}$ **[0/90]s**	$\sigma_{\theta\max}$ **[45/−45]s**	$\sigma_{\theta\max}$ **[0/90]s**	$\sigma_{\theta\max}$ **[45/−45]s**	$\sigma_{\theta\max}$ **[0/90]s**	$\sigma_{\theta\max}$ **[45/−45]s**	$\sigma_{\theta\max}$ **[0/90]s**	$\sigma_{\theta\max}$ **[45/−45]s**
0.4	3.4175	2.0593	3.5515	2.1469	3.7650	2.2889	4.2149	2.5972
0.5	3.4548	2.0836	3.5826	2.1673	3.7870	2.3040	4.2195	2.6004
0.6	3.4354	2.0711	3.5504	2.1462	3.7351	2.2686	4.1290	2.5375
0.7	3.3695	2.0286	3.4658	2.0907	3.6215	2.1928	3.9570	2.4196
0.8	3.2632	1.9614	3.3349	2.0064	3.4519	2.0818	3.7084	2.2511

Table 6: Effect of moisture content on $\sigma_{\theta\max}$

	Laminate	$\sigma_x^{\infty} = 1$		$\sigma_y^{\infty} = 1$		$\sigma_x^{\infty} = \sigma_x^{\infty} = 1$	
		$\sigma_{\theta\max}$	**Angle for** $\sigma_{\theta\max}$	$\sigma_{\theta\max}$	**Angle for** $\sigma_{\theta\max}$	$\sigma_{\theta\max}$	**Angle for** $\sigma_{\theta\max}$
0		3.4548		10.8190		9.8190	
0.1	$[0/90]_{4s}$	3.4593	90° & 270°	10.8373	0° & 180°	9.8373	0° & 180°
0.2		3.4639		10.8557		9.8557	
0		2.0836		5.4013		5.6450	
0.1	$[45/-45]_{4s}$	2.0866	34.5° & 214.5°	5.4094	22.5° & 202.5°	5.6549	25° & 205°
0.2		2.0895		5.4175		5.6649	

Table 7: Fibre material properties [31]

Carbon fibre	**Kevlar fibre**	**S-glass fibre**	**Boron fibre**
$E_{f1} = 220 \times 10^9$ Pa	$E_{f1} = 151.685 \times 10^9$ Pa	$E_{f1} = 85.495 \times 10^9$ Pa	$E_{f1} = 399.896 \times 10^9$ Pa
$E_{f2} = 13.79 \times 10^9$ Pa	$E_{f2} = 151.685 \times 10^9$ Pa	$E_{f2} = 85.495 \times 10^9$ Pa	$E_{f1} = 399.896 \times 10^9$ Pa
$\nu_{f12} = 0.2$	$\nu_{f12} = 0.35$	$\nu_{f12} = 0.2$	$\nu_{f12} = 0.2$
$\alpha_{f1} = -0.99 \times 10^{-6}$m/°C	$\alpha_{f1} = -3.96 \times 10^{-6}$m/°C	$\alpha_{f1} = 3.96 \times 10^{-6}$m/°C	$\alpha_{f1} = 3.96 \times 10^{-6}$m/°C
$\alpha_{f2} = 10.08 \times 10^{-6}$m/°C		$\alpha_{f1} = 3.96 \times 10^{-6}$m/°C	$\alpha_{f1} = 3.96 \times 10^{-6}$m/°C

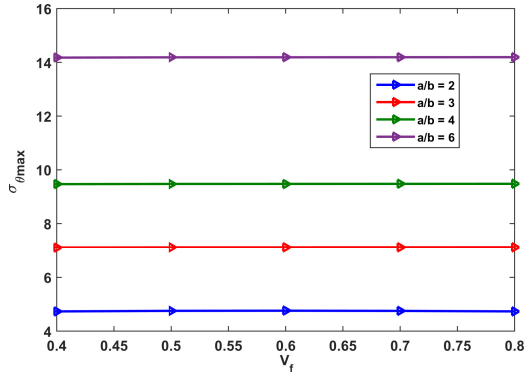

Figure 11: Effect of fibre volume fraction on $\sigma_{\theta\max}$ for ($\sigma_x^{\infty} = 1$, [0/90]s)

Figure 11 shows results $\sigma_{\theta\max}$ for cross ply laminate subjected to tensile loading along x axis for different cases of a/b ratio. From figure it is clear that, change in fibre fraction volume has least effect on the stress concentration. For a/b = 2 & change in Vf from 0.4 to 0.8, there is change of 0.02 % in the stress concentration.

It is important to study the effect of temperature on stress concentration around elliptical hole in laminate plate by choosing different fibre materials. The fibre materials listed in Table 7 are used for the analysis.

Material properties of fiber materials listed in Table 7 are used to study the effect of temperature change on stress concentration for these materials.

Figure 12 shows the distribution of σ_θ around elliptical hole in cross ply laminate plate with four different fibre materials. From Figure 12, it is clear that stress concentration is greatly affected due to material properties. Loading considered for the analysis is tensile along the x axis. We get $\sigma_{\theta\max} = 3.4548$ at 90° & 270° for carbon fibre, $\sigma_{\theta\max} = 3.1329$ at 90° & 270° for Kevlar fibre, $\sigma_{\theta\max} = 2.7197$ at 90° & 270° for S- glass fibre and $\sigma_{\theta\max} = 4.2231$ at 90° & 270° boron fibre.

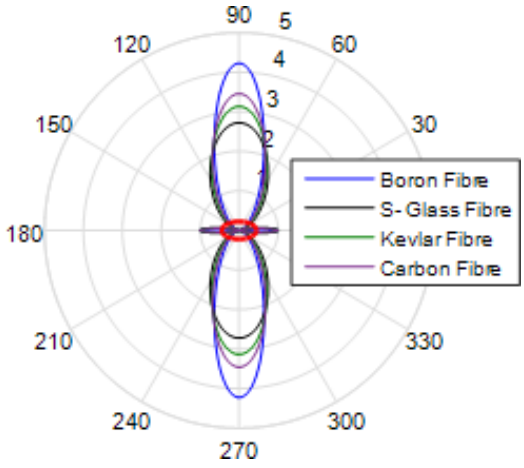

Figure 12: Effect of fibre materials on σ_θ (σ_x^∞ = 1, [0 /90]s)

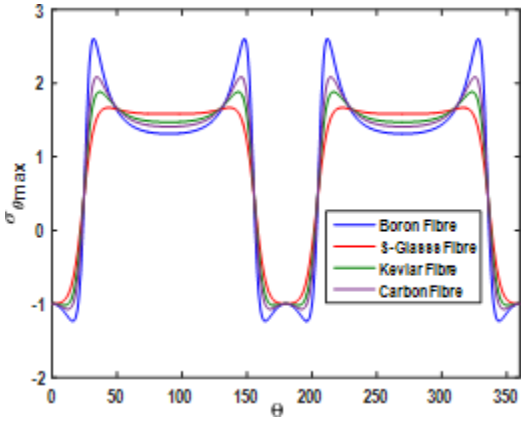

Figure 13: Effect of fibre materials on σ_θ^∞ (σ_x^∞ = 1, [45 /−45]s)

Figure 13 shows the distribution of around elliptical hole in angle ply laminate plate with four different fibre materials. From Figure 13, it is clear that location of $\sigma_{\theta\,\max}$ is different for different materials in ([45/−45]s) laminate plate. Loading considered for the analysis is tensile along the x axis. We get $\sigma_{\theta\,\max}$ = 2.6028 at 32°, 148°, 212° & 328° for carbon fibre, $\sigma_{\theta\,\max}$ = 1.6653 at 43°, 137°, 223° & 317° for Kevlar fibre, $\sigma_{\theta\,\max}$ = 1.8814 at 36.5°, 143.5°, 216.5° & 323.5° S- glass fibre, $\sigma_{\theta\,\max}$ = 2.0836 at 34.5°, 145.5°, 214.5° & 325.5° boron fibre.

From Figure 14 it is clear that change in the temperature has a significant effect on $\sigma_{\theta\,\max}$. Fibre materials differ in thermal coefficient of expansion in longitudinal and transverse direction which reflects in temperature effect on $\sigma_{\theta\,\max}$. If Δt is varied from 0° to 150°, the percentage change in stress concentration is 31%, 28.4%, 23.3% & 32.3% for carbon, Kevlar, S − glass & boron fibres. So elastic modules & thermal coefficient of expansion of fibre material has a significant effect on stress concentration change due to change in temperature of the material.

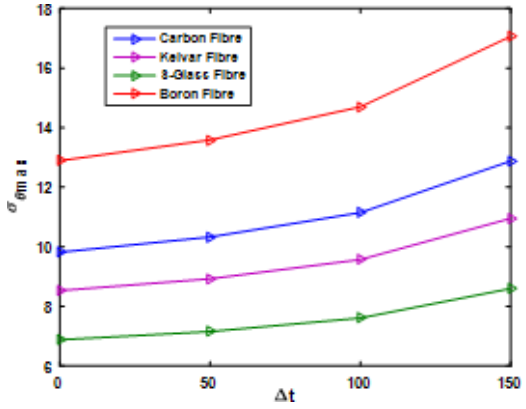

Figure 14: Effect of temperature on $\sigma_{\theta\,\max}$ for different fibre materials (σ_x^∞ = σ_x^∞ = 1, [0 /90]s)

4 Conclusions

This paper presents the solution of stress distribution around elliptical hole in infinite laminate subjected to in plane loading with hygrothermal considerations. Outcomes of the present work can be concluded as:

- The effect of temperature increase on stress concentration is significant for Δt= 100 or above.
- Proper stacking sequence of laminates minimizes the effect of change in temperature on stress concentration.
- The type of the fiber material has significant effect on stress concentration along with the combination of loading condition.
- In cross ply laminate ([0/90]s) with elliptical hole, the stress concentration observed for different loading, materials etc. is higher than the angle ply laminate ([45/−45]s).
- The effect of temperature change on stress concentration is more significant in cross ply laminates as compared with angle ply laminates.
- The Effect of change in moisture content on stress concentration is least significant for all type of loading & stacking sequence.
- The change in stress concentration due to variation in fiber volume fraction is very small.
- a/b ratio affects the stress concentration around elliptical hole.

Funding information: The authors state no funding involved.

Author contributions: All authors have accepted responsibility for the entire content of this manuscript and approved its submission.

Conflict of Interests: The authors state no conflict of interest.

References

[1] Savin GN. Stress Concentration around holes. NY: Pergamon Press. 1961.

[2] Daoust JS, Hoa V. An Analytical Solution for Anisotropic Plates Containing Triangular Holes. Compos Struct. 1991;19(2):107–30.

[3] Gao XL. A general solution of an infinite elastic plate with an Elliptic hole under biaxial loading. J. Press Vessels and Piping. 1996;67(1):95–104.

[4] Simha KR, Mohapatra SS. Stress concentration around irregular holes using complex variable. Sadhana. 1998;23(4):393–412.

[5] Theocaris PS, Petrou L. Stress distributions and intensities at corners of equilateral triangular holes. Int J Fract. 1986;31(4):271–89.

[6] Ukadgaonker VG, Kakhandki V. Stress analysis for an orthotropic plate with an irregular shaped hole for different in-15plane loading conditions—Part 1. Compos Struct. 2005;70(3):255–74.

[7] Rao DK, Ramesh Babu M, Raja Narender Reddy K, Sunil D. Stress around square and rectangular cutouts in symmetric laminates. Compos Struct. 2010;92(12):2845–59.

[8] Rezaeepazhand J, Jafari M. Stress analysis of perforated composite plates. Compos Struct. 2005;71(3-4):463–8.

[9] Sharma DS, Dave JM. Stress intensity factors for hypocycloidal hole with cusps in infinite anisotropic plate. Theor Appl Fract Mech. 2015;75:44–52.

[10] Darwish F, Tashtoush G, Gharaibeh M. Stress concentration analysis for countersunk rivet holes in orthotropic plates. Eur J Mech A, Solids. 2013;37:69–78.

[11] Sharma DS, Patel NP, Trivedi RR. Optimum design of laminates containing an elliptical hole. Int J Mech Sci. 2014;85:3076–87.

[12] Khamseh R, Waas AM. Failure mechanisms of composite plates with a circular hole under remote biaxial planar compressive loads. J Eng Mater Technol. 1997;119(1):56–64.

[13] Sharma DS. Moment distribution around polygonal holes in infinite plate. Int J Mech Sci. 2014;95:131–9.

[14] Li HP, Ellyin F. Determination of stress concentration around an oblique hole by a finite-element technique. J.Vibration Acoustics, Stress. Reliability in Design. 1983;105(2):206–10.

[15] Hasebe N, Irikura H, Nakamura T. A Solution of the Mixed Boundary Value Problem for an Infinite Plate With a Hole Under Uniform Heat Flux. J Appl Mech. 1991;58(4):996–1000.

[16] Puhui C, Zhen S. General solution for an infinite unsymmetric composite laminate containing an Elliptic hole. Mech Res Commun. 2001;28(5):513–8.

[17] Becker W. Complex method for the elliptical hole in an unsymmetric laminate. Appl. Mech. 1993;63:59–169.

[18] Upadhyay AK, Pandey R, Shukla KK. Non-linear flexural response of laminated composite plates under hygro-thermo-mechanical loading. Commun. Non-linear Sci. Numer. Simulat. 2010;15:2634–50.

[19] Kumar R, Patil HS, Lal A. Hygrothermoelastic buckling response of laminated composite plates with random system properties macro-mechanical and micromechanical model. J Aerosp Eng. 2012;28(5):04014123–18.

[20] Lal A, Kulkarni N, Singh BN. Stochastic thermal post-buckling response of elastically supported laminated piezoelectric composite plate using micromechanical approach. Curved Layer Struct. 2015;2(1):331–50.

[21] Pandit MK, Sheikh AH, Singh BN. An improved higher order zigzag theory for the static analysis of laminated sandwich plate with a soft core. Finite Elem Anal Des. 2008;44(9-10):602–10.

[22] Hadjiloizi DA, Kalamkarov AL, Metti C, Georgiades AV. Analysis of Smart Piezo-Magneto-Thermo-Elastic Composite and Reinforced Plates: Part I - Model Development. Curved Layer Struct. 2014;1(1):11–31.

[23] Hadjiloizi DA, Kalamkarov AL, Metti C, Georgiades AV. Analysis of Smart Piezo-Magneto-Thermo-Elastic Composite and Reinforced Plates: part II – Applications. Curved Layer Struct. 2014;1(1):32–58.

[24] Hsieh MC, Hwu C. Hygrothermal Stresses in Unsymmetric Laminates Disturbed by Elliptical Holes, ASME. J Appl Mech. 2006;73(2):228–39.

[25] Saeed R, Roham R, Maleki M. The influence of hygrothermal environments on the stress concentration in unidirectional composite lamina. Mech Mater. 2019;129:332–40.

[26] Sai Ram KS, Sinha PK. Hygrothermal bending of laminated composite plate without hole. Comp. Struct. 1992;43(6):1105–15.

[27] Dimitri R, Fantuzzi N, Tornabene F, Zavarise G. Innovative numerical methods based on SFEM and IGA for computing stress concentrations in isotropic plates with discontinuities. Int. J. Mech. Sci. (NY). 2016;118:166–87.

[28] Fantuzzi N, Dimitri R, Tornabene F. A SFEM-based evaluation of mode-I Stress Intensity Factor. Comp. Struct. 2016;145:162–85.

[29] Viola E, Tornabene F, Fantuzzi N, Bacciocchi M. Numerical Investigation of Composite Materials with Inclusions and Discontinuities. Key Eng Mater. 2017;747:69–76.

[30] Jones R. Mechanics of Composite Material. Washington (D.C.): Mcgraw-Hill Ko-gakusha Ltd. 2002.

[31] Gibson RF. Principles of Composite Material Mechanics. CRC-press. 2016.

[32] Muskhelishvili NI. Some basic problems of the mathematical theory of elasticity. P.Noordhooff Ltd. Groningen: The Netherlands. 1963.